Ebola Virus Enters Host Cells by Macropinocytosis and Clathrin-Mediated Endocytosis

Paulina Aleksandrowicz,[1,2,3] Andrea Marzi,[4] Nadine Biedenkopf,[5] Nadine Beimforde,[1] Stephan Becker,[5] Thomas Hoenen,[5] Heinz Feldmann,[4,6] and Hans-Joachim Schnittler[1]

[1]Institute of Anatomy and Vascular Biology, Westfälische Wilhelms University Muenster, Vesaliusweg, [2]Institute of Physiology, and [3]MTZ Imaging Facility, University of Technology Dresden, Germany; [4]Laboratory of Virology, Division of Intramural Research, National Institute of Allergy and Infectious Diseases, National Institutes of Health, Rocky Mountain Laboratories, Hamilton, Montana; [5]Philipps University Marburg, Institute of Virology, Germany; and [6]Special Pathogens Program, National Microbiology Laboratory, Public Health Agency of Canada, Winnipeg, Canada

Virus entry into host cells is the first step of infection and a crucial determinant of pathogenicity. Here we show that Ebola virus-like particles (EBOV-VLPs) composed of the glycoprotein $GP_{1,2}$ and the matrix protein VP40 use macropinocytosis and clathrin-mediated endocytosis to enter cells. EBOV-VLPs applied to host cells induced actin-driven ruffling and enhanced FITC-dextran uptake, which indicated macropinocytosis as the main entry mechanism. This was further supported by inhibition of entry through inhibitors of actin polymerization (latrunculin A), Na^+/H^+-exchanger (EIPA), and PI3-kinase (wortmannin). A fraction of EBOV-VLPs, however, colocalized with clathrin heavy chain (CHC), and VLP uptake was reduced by CHC small interfering RNA transfection and expression of the dominant negative dynamin II–K44A mutant. In contrast, we found no evidence that EBOV-VLPs enter cells via caveolae. This work identifies macropinocytosis as the major, and clathrin-dependent endocytosis as an alternative, entry route for EBOV particles. Therefore, EBOV seems to utilize different entry pathways depending on both cell type and virus particle size.

Ebola viruses (EBOVs), belonging to the family *Filoviridae*, are enveloped, nonsegmented, negative-stranded RNA viruses that can cause severe viral hemorrhagic fevers in human and nonhuman primates with case fatality rates for humans of up to 90% [1]. Many cell types seem to be susceptible to EBOV infection, but lymphocytes are known to be resistant [2, 3]. Free access of circulating virus to monocytes/macrophages, dendritic cells, and hepatocytes may be a key factor in defining primary target cells and subsequently target organs for EBOV [4].

EBOV particles acquire their envelope from the host cell plasma membrane during the budding process. Particles possess a single trimeric transmembrane glycoprotein ($GP_{1,2}$) that mediates virus uptake through receptor binding and subsequent fusion [5]. Certain cellular molecules have been identified to enhance EBOV infection such as β1 integrins [6], dendritic cell–specific ICAM-3 grabbing nonintegrin (DC-SIGN) and its homologue DC-SIGNR [7], and Axl receptor tyrosine kinase [8]. In addition, the asialoglycoprotein receptor (ASGP-R) has been identified as a potential receptor for Marburg virus (MARV) [9]. However, none of these molecules is essential for EBOV and MARV entry, and no receptor for filoviruses has been identified yet.

Since EBOV, like other viruses, is an obligatory intracellular parasite, its replication cycle critically depends on host cell functions and requires delivery of the viral genome into target cells. Uptake of virus particles can occur via different types of cell-dependent endocytotic mechanisms (for a review, see [10]). Eukaryotic endocytotic processes range from highly specific uptake of soluble ligands via clathrin-coated pits to uptake of large particles including apoptotic cells via macropinocytosis or phagocytosis [11]. Several attempts were

Potential conflicts of interest: none reported.

Correspondence: Hans-Joachim Schnittler, MD, PhD Institut für Anatomie und Vaskulaere Biologie, Westfälische Wilhelms-Universität Münster, Vesaliusweg 2 – 4, 48149 Münster (hans.schnittler@uni-muenster.de).

The Journal of Infectious Diseases 2011;204:S957–S967

0022-1899 (print)/1537-6613 (online)/2011/204S3-0030$14.00
DOI: 10.1093/infdis/jir326

made to identify the mechanism of EBOV uptake. Human immunodeficiency virus (HIV) particles pseudotyped with EBOV-$GP_{1,2}$ were shown to colocalize with caveolin-1, and their entry was dependent on clathrin and membrane lipid composition, as removal or clustering of cholesterol affected infection [12, 13]. Infection of EBOV-pseudotyped lentivirus particles and EBOV was also impaired by inhibitors of clathrin-mediated endocytosis and several other endocytotic pathways [14, 15]. Recent reports show that actin-dynamics, intact microtubules, and the involvement of the class I phosphatidylinositol-3 kinase (PI3K)–Akt pathway are critical for EBOV uptake [13, 15, 16]. However, the size of EBOV particles, which have a uniform diameter of 80 nm, varies dramatically in length ranging from 600 to 1 400 nm, and peak infectivity is associated with 805-nm particles [17]. Thus, the morphology of EBOV particles argues against host cell entry by caveolae (typical for particle sizes ranging from 50 to 100 nm) [18] or "canonical" clathrin-coated pits (typical for particle sizes <200 nm) [19].

We propose that EBOV entry occurs mainly by macropinocytosis, an endocytotic mechanism that allows the uptake of large particles. To address this hypothesis, we utilized 2 surrogate systems for infectious EBOV, EBOV-like particles (EBOV-VLPs) [20, 21] and the advanced "infectious" VLPs (EBOV-iVLPs) [22]. Using immunofluorescence, small interfering RNA (siRNA) silencing, and inhibition of specific host cell signaling and cytoskeleton rearrangement, we demonstrated that EBOV particle entry into host cells mainly followed the characteristics of macropinocytosis. In addition, we found that a smaller fraction of particles entered via clathrin-mediated endocytosis.

MATERIALS AND METHODS

Materials

Latrunculin A and wortmannin were obtained from Calbiochem; 5-(*N*-Ethyl-*N*-isopropyl)-amiloride (EIPA) from Alexis Biochemicals; and phorbol 12-myristate 13-acetate (PMA), phalloidin-TRITC, phalloidin–fluorescein isothiocyanate (FITC), and 4.2 kDa FITC-dextran from Sigma-Aldrich. Dextran-FITC 70 kDa, human transferrin–Alexa Fluor 546, FITC, and cholera toxin B–Alexa Fluor 488 were purchased from Invitrogen. Cy5-NHS ester was purchased from GE Healthcare, and plastic dishes for microscopy were from Ibidi. Fugene 6 was obtained from Roche, and TurboFect from Fermentas. The rabbit polyclonal antibody against caveolin-1 was purchased from Santa Cruz Biotechnology, and mouse monoclonal antibodies against clathrin heavy chain (CHC) and early endosome antigen 1 (EEA1) were purchased from BD Transduction. The mouse monoclonal antibody against α-tubulin was obtained from Sigma-Aldrich, and the rabbit polyclonal antibody against dynamin II from Abcam. The goat polyclonal antibody against the enhanced green fluorescent protein (EGFP) was generated in the Antibody Facility of the Max Planck Institute of Cell Biology and Genetics. The mouse monoclonal antibody against EBOV glycoprotein (GP) and the rabbit polyclonal antibody against EBOV VP40 were provided by Dr Yoshihiro Kawaoka, University of Wisconsin. Stock solutions (1000×) of all the drugs were dissolved in endotoxin-free dimethyl sulfoxide (DMSO) (Sigma-Aldrich). Control cells were treated with medium containing 0.1% DMSO.

Cell Culture and Immunofluorescence Experiments

HeLa, 293T, and Vero E6 cells were cultured in Dulbecco's modified Eagle's medium–GlutaMAX (Invitrogen) supplemented with 10% fetal calf serum, penicillin (100 U/mL), and streptomycin (100 μg/mL) under standard culture conditions at 37°C and 7.5% CO_2. For immunofluorescence (IF) analysis, cells were grown on glass-bottom dishes (house-made) coated with cross-linked gelatin or on plastic culture dishes, fixed with either 2% or 4% formaldehyde, permeabilized with 0.1% Triton X-100 at 4°C, washed with phosophate-buffered saline (PBS), blocked with 1% bovine serum albumin (BSA) for 1 hour, and subsequently incubated with the respective primary and secondary antibodies and mounted in mounting medium (60% glycerol, 40% water, N-propyl gallate) as described elsewhere [23]. DAPI (0.2 μg/mL) or phalloidin-TRITC or phalloidin-FITC (0.4 μg/mL) was applied to the cells during incubation with the secondary antibody.

Drug Treatment

HeLa and Vero E6 cells were pretreated in serum-free medium with 0.5μM latrunculin A (actin polymerization inhibitor) for 90 minutes, 100 nM wortmannin (PI3K inhibitor) for 60 minutes, and 25–200 μM EIPA (5-(*N*-Ethyl-*N*-isopropyl)-amiloride, an inhibitor of the Na^+/H^+-exchanger [NHE]) for 30 minutes, followed by infection with either EBOV-iVLPs or *Zaire ebolavirus* expressing enhanced green fluorescent protein (ZEBOV-EGFP). For determination of luciferase activity, EBOV-iVLPs were left on the cells for 90 minutes followed by replacement with 5% FCS-containing medium. Wortmannin and latrunculin A were still present in the medium for another 4 hours to avoid EBOV-iVLP entry after drug removal.

Generation of EBOV-VLPs, EBOV-iVLPs, and ZEBOV-EGFP

EBOV-VLPs were generated through expression of ZEBOV $GP_{1,2}$ and VP40 as described previously [21]. EBOV-iVLPs containing all structural ZEBOV proteins and a minigenome expressing *Renilla* luciferase were generated as described elsewhere [22]. ZEBOV-EGFP was produced as described before [24].

Labeling EBOV-VLPs or EBOV-iVLPs With FITC or Cy5

Particle labeling was performed as described by Helenius et al [25] with modifications. In brief, VLPs were suspended in 0.1 bicarbonate buffer pH 8.3 at a concentration of 0.5 mg/mL protein and labeled for 1 hour with a fluorescent dye at room

temperature. The unbound dye was removed by dialysis against PBS using Slide-A-Lyser dialysis cassette (Thermo Scientific).

Cloning of Caveolin-1-mCherry and Caveolin-1-EGFP Into a Lentiviral Vector and Gene Transduction

Human caveolin-1-mCherry WT was amplified using forward primer TAG CTA GCC ACC ATG TCT GGG GGC AAA TAC GTA and reverse primer GGC GGT ACC ACT ATT TCT TTC TGC AAG TTG ATG CG, and inserted into the pmCherry-N1 plasmid (Clontech Laboratories) using NheI and KpnI restriction sites. The plasmid, caveolin-1-EGFP, was described previously [26]. Both versions of caveolin-1 were cloned into the lentiviral vector pFUGW (kindly provided by Yvan Arsenijevic, Lausanne, Switzerland), and lentiviruses were produced and gene transfer was performed as described previously [27, 28].

siRNA Transfection

Dynamin II-WT (wild-type) and dynamin II-K44A fused with mCherry were kindly provided by A. Helenius (Zuerich, Switzerland) [29]. HeLa cells were transfected with dynamin II constructs using TurboFect according to the manufacturer's instructions (Fermentas) and cultured for 40 hours prior to treatment. Downregulation of CHC was performed by siGENOME SMARTpool siRNA nucleotides. Nontargeting siRNA Pool #1 (Dharmacon) was used as a negative control. A mixture of siRNA sequences consisting of (1) GAA AGA AUC UGU AGA GAA A, (2) GCA AUG AGC UGU UUG AAG A, (3) UGA CAA AGG UGG AUA AAU U, and (4) GGA AAU GGA UCU CUU UGA A targeting the CHC was applied to the cells at a final concentration of 50 μg/well in a 12-well plate.

Fluorescence-Activated Cell Sorting

For FACS analysis, cells were trypsinized, kept on ice in buffer (5% FCS, 2 mM EDTA, PBS), and subsequently analyzed using a FACSCalibur (Becton Dickinson). For positive controls, cells were treated with 200 mM PMA during the entire experiment. Mean fluorescence intensity was measured in each sample, and results were normalized to the negative control.

Internalization Assays for VLPs, Transferrin, and FITC-Dextran

Serum-starved HeLa or Vero cells were cooled to 4°C and incubated for 1 hour with EBOV-VLPs, EBOV-iVLPs, or EBOV-iVLP-Cy5. A temperature shift to 37°C was performed after washing with PBS using prewarmed (37°C) serum-free medium containing 0.2% BSA for the indicated time intervals, and cells were further processed for immunofluorescence or FACS analysis. For transferrin uptake, cells were exposed to transferrin–Alexa Fluor 546 at 37°C 15 minutes before fixation, washed with glycin buffer (0.1 M glycin, 0.1 M NaCl, pH 3.0), and further processed for immunofluorescence analyses. For fluid-phase uptake, cells were exposed to either 0.5 mg/mL 4.2 kDa FITC-dextran for the last 10 minutes or 1 mg/mL 70 kDa FITC-dextran for the last 5 minutes at 37°C before collection at indicated time points. Cells were placed on ice and washed with PBS, and surface-bound FITC-dextran was bleached by low pH buffer (0.1 M sodium acetate, 0.05 M NaCl, pH 5.5) prior to processing for IF or FACS analysis.

EBOV-iVLP Assay

For determination of luciferase activity expressed by EBOV-iVLPs, serum-starved cells (for 4 hours) were infected with EBOV-iVLPs in serum-free medium for 90 minutes followed by the addition of medium containing 5% FCS and incubated for a further 70 hours. Luciferase activity was determined using the *Renilla* Luciferase assay kit according to the manufacturer's instructions (Promega).

Live Cell Imaging

HeLa cells were cultured for 48 hours and incubated with either EBOV-VLPs-FITC or EBOV-VLPs-Cy5 for 1 hour at 4°C, washed with PBS at 4°C, and investigated by live cell imaging at 37°C. Time lapse recording was performed 3-dimensionally for up to 1 hour using a Leica TC SP5 microscope equipped with a 40×/1.2 water immersion objective.

Infection of Cells With ZEBOV-EGFP

ZEBOV-EGFP infection was performed with a multiplicity of infection (MOI) of 1 for 1 hour followed by replacement with fresh medium containing 5% FCS. After 24 hours' incubation at 37°C and 5% CO_2, the number of GFP-positive cells was

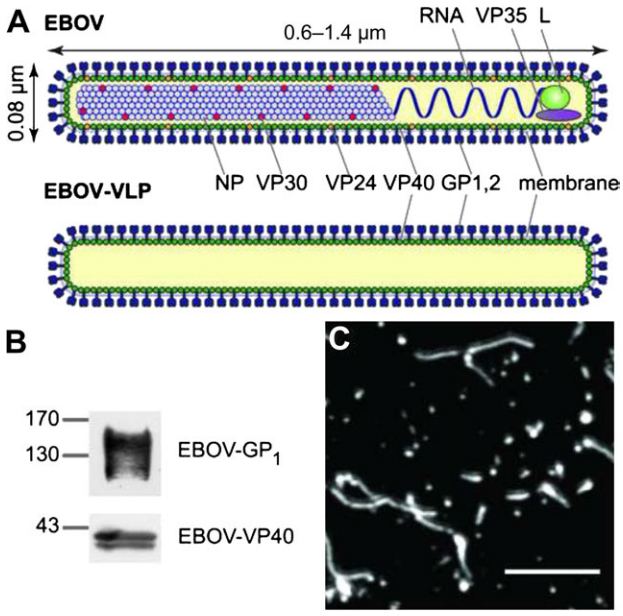

Figure 1. Ebola viruses (EBOVs) and Ebola virus-like particles (EBOV-VLPs). *A,* A scheme of EBOV and EBOV-VLPs illustrating the overall organization. The minimal components of EBOV-VLPs are the glycoprotein $GP_{1,2}$ on the surface and the matrix protein VP40, which is needed for particle formation. *B,* Western blot analysis of EBOV-VLPs showing the presence of GP_1, the larger cleavage fragment, and VP40. *C,* EBOV-VLPs stained for EBOV-$GP_{1,2}$. EBOV-VLPs are similar in morphology to infectious EBOV. Scale bar: 2 μm.

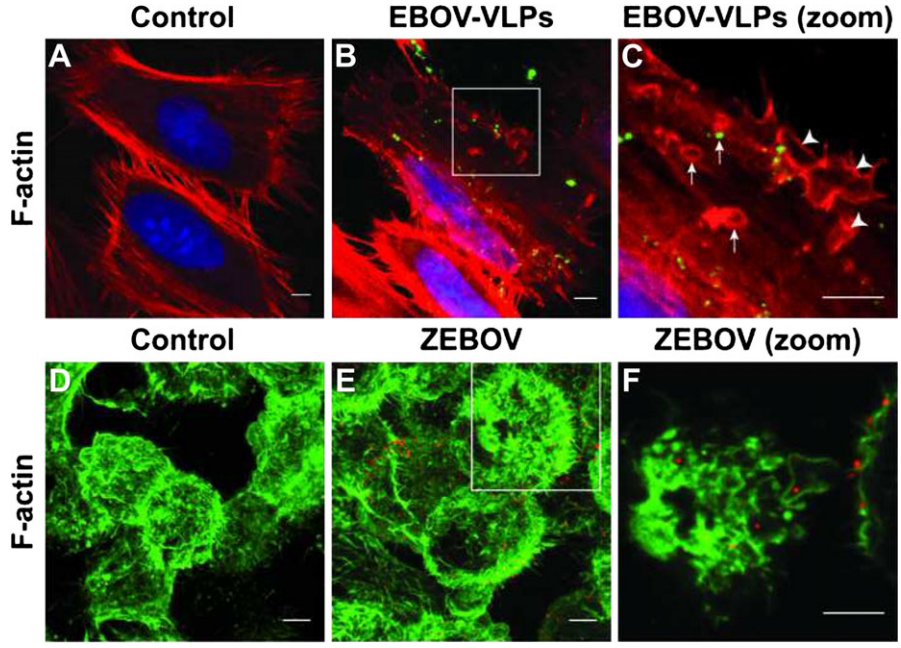

Figure 2. Ebola virus-like particles (EBOV-VLPs) and *Zaire ebolavirus* (ZEBOV) induce formation of actin ruffles and macropinosomes. *A–C,* HeLa cells were exposed to EBOV-VLPs or phosphate-buffered saline (control) for 30 minutes, and fixed with formaldehyde. Actin filaments were labeled with phalloidin-TRITC (*red*) and EBOV-VLPs with a $GP_{1,2}$-specific antibody (*green*). Higher magnification of the boxed area reveals actin ruffles (arrowheads) and macropinosomes (arrows) with and without EBOV-VLPs. *D–F,* Formaldehyde-fixed HeLa cells, 15 minutes after exposure to ZEBOV (multiplicity of infection = 1), were stained for filamentous actin with phalloidin–fluorescein isothiocyanate (FITC) (*green*) and for EBOV with antibody against EBOV-VP40 (*magenta*). Higher magnification of the boxed area reveals virus particles engulfed by actin ruffles and inside macropinosomes. Experiments were repeated 3 times with similar results.

determined by FACS analysis. For immunofluorescence studies, serum-starved Vero E6 cells were exposed to infectious ZEBOV (MOI of 1) at 4°C and incubated for 1 hour. The temperature shift was performed after washing with PBS using prewarmed (37°C) serum-free medium containing 0.2% BSA for the indicated time intervals. Cells were fixed and inactivated with 4% paraformaldehyde according to standard operating procedures for Biosafety Level 4 approved by the Institutional Biosafety Committee (National Institute of Allergy and Infectious Diseases, National Institutes of Health, Rocky Mountain Laboratories, Hamilton, Montana).

Image Acquisition and Analysis

Images were acquired using a laser scanning confocal microscope (Zeiss LSM 510), equipped with a Plan Apochromat 63×/1.4 oil immersion objective. Images used in the manuscript were processed using Fiji [30]. For colocalization analysis at each time point, 3–5 fields per sample were randomly selected with 2–5 cells per visual field. Object-based colocalization of EBOV-VLPs and respective endocytotic structures was quantified using Motion Tracker software [31] on unprocessed images. In brief, the fluorescent-labeled structures were recognized as objects and their overlap by more than 50% was scored as a positive result. The percentage of VLPs that colocalized with endocytotic structures was quantified in at least 3 independent experiments.

RESULTS

To test whether EBOV-VLPs use macropinocytosis as an entry route into target cells, we used different experimental approaches. Macropinocytosis is characterized by formation of macropinosomes, which are structures of eukaryotic plasma membranes ranging in size from 0.2 to 10 μm. It occurs spontaneously or in response to stimulation by growth factors or by PMA-mediated protein kinase C activation to engulf extracellular fluid for cellular uptake [11]. This process requires actin-driven ruffle formation, PI3K activation, and NHE activity [11].

EBOV-VLPs Induce Actin-Driven Ruffling and Increased Fluid Uptake

EBOV-VLPs were generated by transfection of 293 T cells with plasmids encoding for the EBOV- $GP_{1,2}$ and matrix protein VP40 [20, 21], resulting in particles of about 80 nm in diameter and a length of up to 2 μm [32], similar to authentic EBOV (Figure 1). Western blot and immunofluorescence analyses confirmed the presence of the basic components of purified EBOV-VLPs: $GP_{1,2}$ and VP40 (Figure 1). Administration of EBOV-VLPs to HeLa cells induced actin-driven membrane ruffling at the cell surface leading to large vesicles (0.5 -3.5 μm in diameter) over the entire cell body, many of which contained EBOV-VLPs (Figure 2). This indicates that EBOV-VLPs stimulate membrane ruffling, a process characteristic for macropinocytosis [10]. These

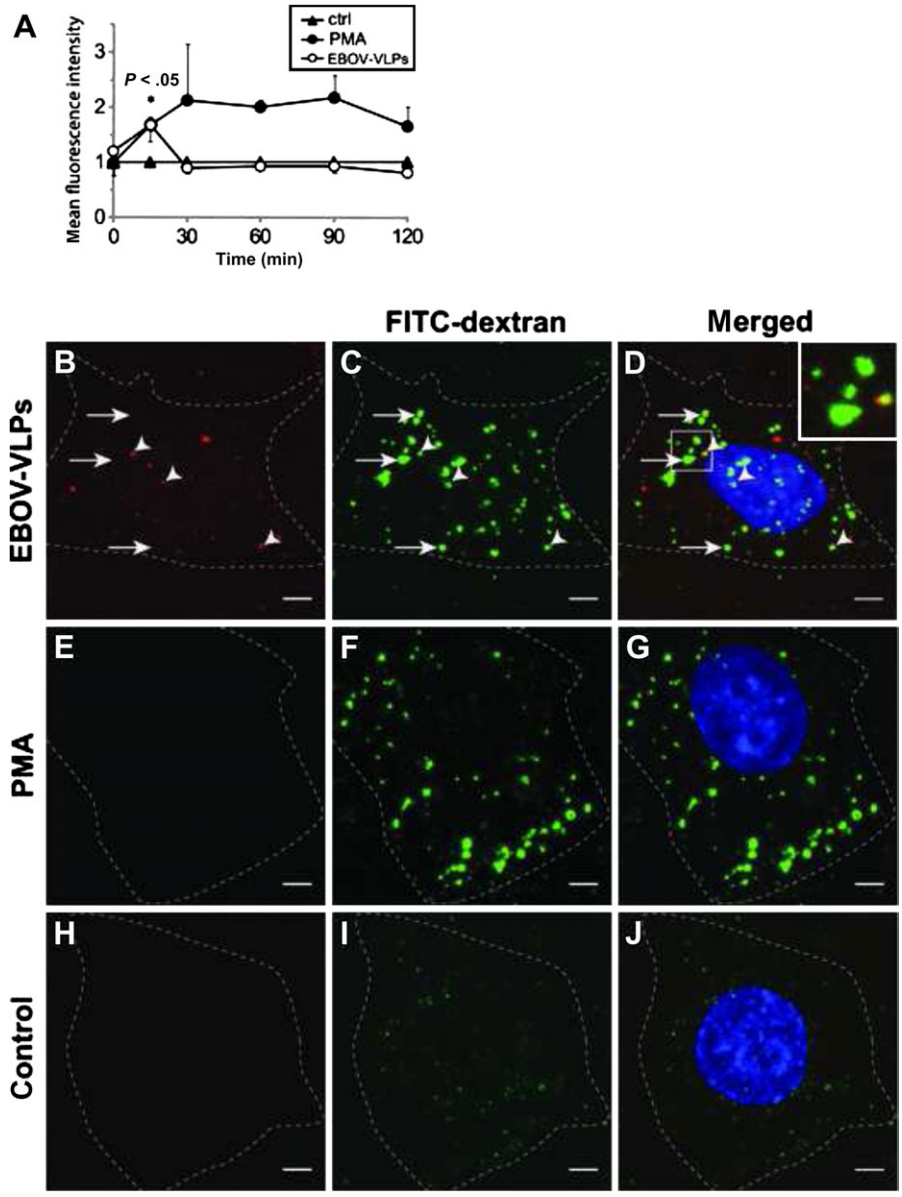

Figure 3. Ebola virus-like particles (EBOV-VLPs) stimulate fluid-phase macropinocytosis in Vero and HeLa cells. *A*, EBOV-VLPs were bound to Vero E6 cells on ice, shifted to 37°C for the indicated time periods, exposed for fluorescein isothiocyanate (FITC)–dextran during the last 10 minutes, and analyzed by fluorescence-activated cell sorting. Phorbol 12-myristate 13-acetate (PMA) (200 nM) served as a positive control. EBOV-VLPs increased the FITC-dextran uptake transiently. *B–D*, Addition of EBOV-VLPs-Cy5 (*red*) and FITC-dextran (*green*); or *E–G*, 200 nM PMA and FITC-dextran (*green*); or *H–J*, only FITC-dextran (*green*) to HeLa cells 30 minutes after temperature shift to 37°C. Both EBOV-VLPs-Cy5 and PMA (used as positive control) stimulate uptake of fluid phase as indicated by FITC-dextran-positive macropinosomes. Dotted lines indicate cell borders. FITC-dextran (*green*); EBOV-VLP-Cy5 (*red*); nuclei labeled with DAPI (*blue*). Experiment was repeated 4 times. Bars in *A* represent standard errors. Scale bar: 5 μm.

results were confirmed in experiments with infectious EBOV, in which many virus particles were surrounded by actin ruffles and found within vesicles (Figure 2). To quantitatively determine EBOV-VLP–induced macropinocytosis, the uptake of fluid-phase marker FITC-dextran was measured by FACS analysis. FITC-dextran uptake increased by 68% over constitutive baseline level within 15 minutes after administration of EBOV-VLPs, and returned to baseline within 30 minutes (Figure 3). Administration of PMA (positive control) doubled fluid-phase uptake over the treatment period (Figure 3). These observations were further confirmed by visualization of dextran-filled vesicles upon stimulation with Cy5-labeled EBOV-VLPs (EBOV-VLP-Cy5). Application of EBOV-VLP-Cy5 increased the number of vesicles in both HeLa (Figure 3) and VeroE6 cells (Supplementary Figure 1). EBOV-VLPs colocalized with FITC-dextran inside vesicles in both cell types. PMA also increased the number of FITC-dextran–positive vesicles (Figure 3), while untreated cells remained at baseline

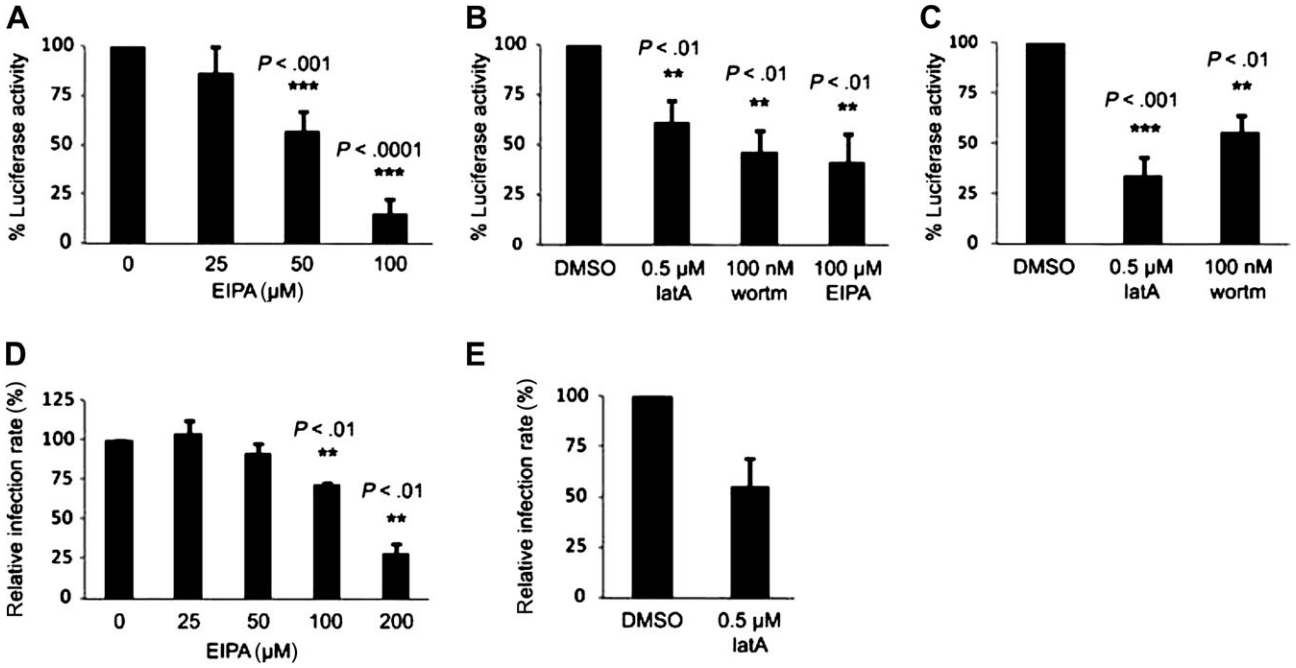

Figure 4. Inhibitors of macropinocytosis block Ebola infectious virus-like particle (EBOV-iVLP) infection and uptake of recombinant Ebola virus (EBOV). HeLa cells and Vero E6 cells were treated with 5-(*N*-Ethyl-*N*-isopropyl)-amiloride (EIPA) (up to 200 μM), latrunculin A (0.5 μM), or 100 nM wortmannin prior to infection. *A*, HeLa cells exposed to EIPA were infected with EBOV-iVLPs leading to the expression of *Renilla* luciferase, which was dose-dependently inhibited by EIPA. *B* and *C*, EIPA, latrunculin A, and wortmannin decreased EBOV-iVLP infection in both cell types. *D* and *E*, Vero E6 cells were treated with either EIPA or latrunculin as indicated and subsequently infected with infectious *Zaire ebolavirus*–green fluorescent protein (ZEBOV-GFP). Inhibition of enhanced green fluorescent protein (EGFP) expression was seen for EIPA and latrunculin. Each experiment with EBOV-iVLPs was repeated 4–7 times. Experiments with infectious EBOV-EGFP were repeated 3 times. Error bars represent standard errors. *P* values indicate significance. DMSO, dimethyl sulfoxide.

levels (Figure 3). Taken together, these findings indicate that attachment of EBOV-VLPs induces macropinocytosis over a large portion of the cellular plasma membrane by actin-mediated ruffle formation.

Inhibitors of Macropinocytosis Block EBOV-iVLP Infection

To further confirm that macropinocytosis is an uptake pathway for EBOV-VLPs, we investigated the impact of drugs that block signaling and host cell mechanisms critical for macropinocytosis on the uptake of EBOV-VLPs. The drugs tested included: (1) latrunculin A, a sponge toxin that stoichiometrically binds to actin monomers and blocks actin polymerization [33]; (2) 5-(*N*-Ethyl-*N*-isopropyl)-amiloride, an inhibitor of the Na^+/H^+-exchanger [34]; and (3) wortmannin, a fungal toxin that at low concentrations specifically inhibits PI3-kinase [35]. To quantitatively analyze the impact of these inhibitors on EBOV-VLP uptake, we generated EBOV-iVLPs containing a minigenome with a reporter gene encoding for *Renilla* luciferase [22]. EIPA inhibited EBOV-iVLP–induced luciferase expression in HeLa cells in a dose-dependent manner, and Vero E6 cells were also sensitive to this inhibitor (Figure 4). Significant inhibitory effects on EBOV-iVLP uptake were also observed in HeLa and Vero E6 cells treated with latrunculin A and wortmannin (Figure 4). To further confirm the drug inhibitory effects on EBOV infectivity, we used recombinant ZEBOV-EGFP. Both EIPA and latrunculin A inhibited GFP expression in Vero E6 cells induced by ZEBOV-EGFP infection (Figure 4). Together, the data identify macropinocytosis as an important pathway for EBOV particle uptake.

Clathrin Contributes to EBOV-VLP Uptake

Viruses have been shown to use different pathways for entering host cells, including clathrin-mediated endocytosis [10], a mechanism that has also been suggested for EBOV [14, 15]. Therefore, we directly tested the impact of clathrin on EBOV-iVLP uptake by siRNA-mediated downregulation of the CHC. CHC-siRNA downregulated clathrin by 75% in HeLa cells, as determined by quantitative Western blot analysis (Figure 5). In clathrin-depleted cells, EBOV-iVLP infection was reduced as indicated by a 25% reduction of luciferase reporter activity (Figure 5). This effect is consistent with a transient colocalization of EBOV-VLPs and clathrin (Figure 5) and the appearance of EBOV-VLPs (~20%) in early endosomes 30 minutes after the temperature shift from 4°C to 37°C as demonstrated by colocalization with EEA1 (Figure 5). Transferrin, which served as positive control for clathrin-mediated uptake (Figure 5), largely colocalized with EEA1 in the early endosome as well (Figure 5). These results indicate that productive entry of EBOV-VLPs into

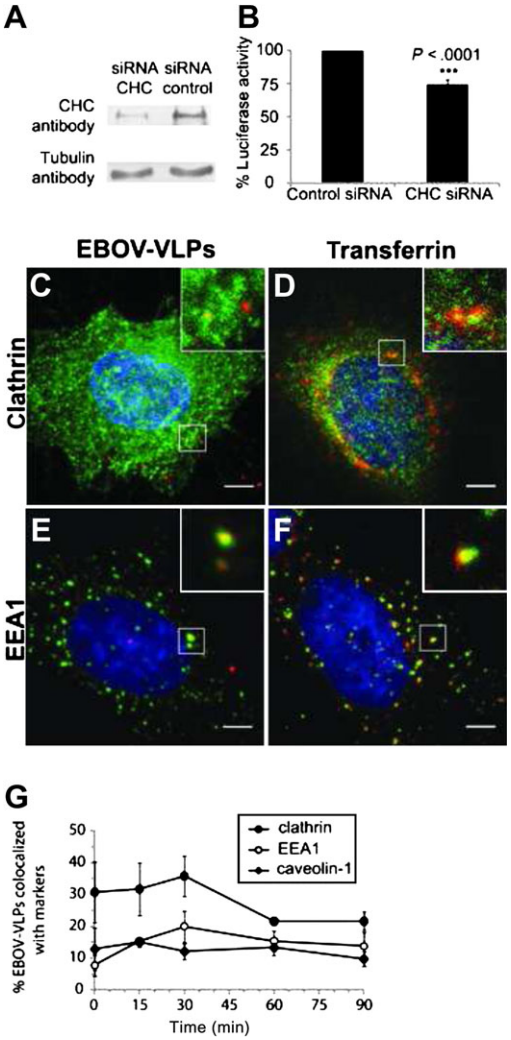

Figure 5. Clathrin modulates Ebola infectious virus-like particle (EBOV-iVLP) entry into HeLa cells. *A*, Downregulation of clathrin heavy chain (CHC) in HeLa cells by small interfering RNA (siRNA), as shown by Western blotting. *B*, Clathrin-depleted HeLa cells and control cells were infected with EBOV–iVLPs that mediate expression of *Renilla* luciferase, which was used as readout for infectivity. Despite a 75% downregulated CHC, the reduction of EBOV-iVLP infection was only 25%. *C* and *D*, Virus-like particle (VLP) adsorption was performed for 1 hour at 4°C followed by a 15-minute temperature shift to 37°C. Colocalization of VLPs (stained with anti-EBOV-VP40 antibody) with either clathrin or early endosome antigen 1 (EEA1), and transferrin with clathrin or EEA1 was determined by immunofluorescence analysis. *G*, Quantification of VLPs colocalized with clathrin, EEA1, or caveolin-1 at indicated time points. Data are based on 3 independent experiments. Error bars represent standard errors. Scale bar: 5 μm.

host cells also depends on the clathrin-mediated endocytotic pathway.

Caveolin-1 Does Not Colocalize With EBOV-VLP During Uptake

Caveolin-1 is the main scaffolding protein of caveolae, which are small plasma membrane invaginations of about 80 nm in diameter that have signaling functions for a wide variety of cellular mechanisms including endocytotic processes [36]. Caveolin-1 is a characteristic protein of cholesterol- and sphingolipid-rich, detergent insoluble plasma membrane domains (rafts) [36]. Because extraction and clustering of cholesterol had an impact on EBOV uptake [37], we wondered if also caveolin-1 might be a critical molecule in this process. We expressed caveolin-1-mCherry and caveolin-1–EGFP fusion proteins in cells and performed live cell imaging to directly follow the fate of EBOV-VLP-FITC or EBOV-VLP-Cy5. Both caveolin-1 fusion proteins behaved similarly and showed colocalization with endogenous caveolin-1 (Figure 6). Application of EBOV-VLP-Cy5 to cells expressing caveolin-1–EGFP resulted in uptake of VLPs within 20–30 minutes, but colocalization was hardly detectable over the recorded time period (Figure 6). This is consistent with only limited colocalization of $GP_{1,2}$ (a component of EBOV-VLPs) with caveolin-1, as demonstrated by double immunostaining (Figure 6). These data indicate that at least in HeLa cells, EBOV particle entry is independent on caveolin-1/caveolae.

Dynamin II Has a Moderate Impact on EBOV-VLP Uptake

Dynamin II is a large GTPase essential for both clathrin-coated pits and caveolae-mediated endocytosis that acts by pinching off the preformed vesicles from the membrane. It also participates in formation of podosomes and invadopodia [38], and has been proposed to modulate Rac1 localization [39]. However, scission of macropinosomes from the plasma membrane is supposed to be largely dynamin II independent [40]. Expression of dynamin II-WT and dynamin II-K44A, a dominant negative mutant, was achieved by either classical transfection technology or by adenovirus gene transfer (for a review, see [41]). As a control we used transferrin, which binds to the transferrin receptor and is typically taken up by classical clathrin-mediated endocytosis [42]. Dynamin II-K44A expression in HeLa cells downregulated the EBOV-iVLP–mediated luciferase activity by 25% (Figure 7), indicating a moderate role of dynamin II on particle entry. Overexpression of dynamin II-WT in unmodified cells or cells expressing dynamin WT showed transferrin-positive vesicles after a temperature shift from 4°C to 37°C (Figure 7). In contrast, transferrin uptake was completely blocked in cells expressing the dominant negative mutant, demonstrating the inhibitory effect of dynamin II-K44A (Figure 7). Coapplication of EBOV-VLPs and transferrin to cells expressing dynamin II-WT revealed that only 20% of EBOV-VLPs colocalized with transferrin in large vesicles (Figure 7; Supplementary Figure 2). Expression of dynamin II-K44A completely blocked transferrin uptake but not the uptake of EBOV-VLPs (Figure 7). Together, the 20% colocalization of EBOV-VLPs with both clathrin (Figure 5) and transferrin (Figure 7) and the 25% inhibition of EBOV-VLP uptake after expression of dynamin II-K44A mutant (Supplementary Figure 2) clearly indicate that a portion of EBOV-VLPs uses clathrin-mediated endocytosis as the uptake mechanism.

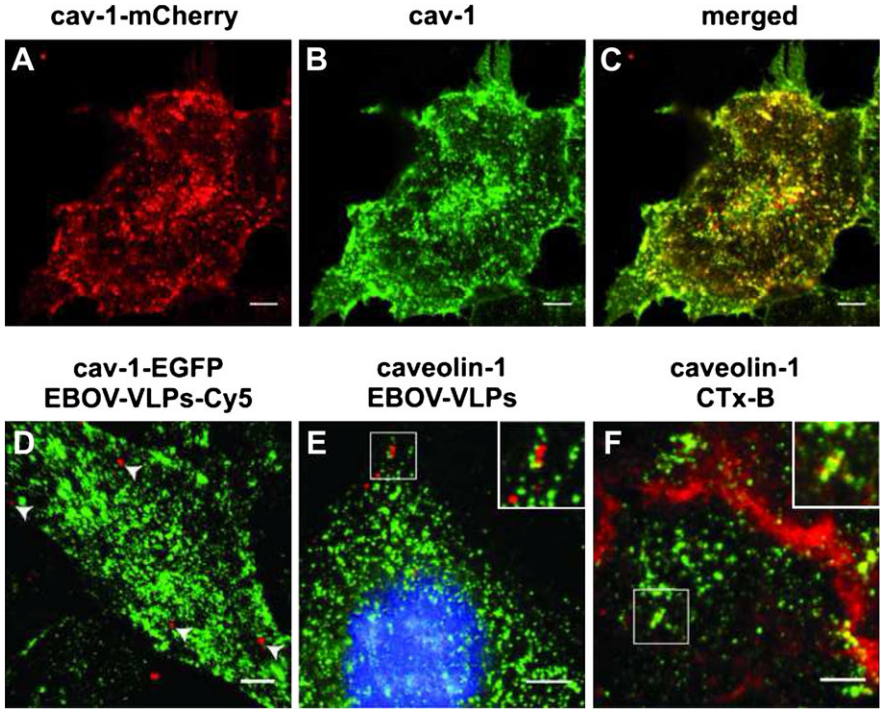

Figure 6. Ebola virus-like particles (EBOV-VLPs) do not colocalize with caveolin-1 in HeLa cells. *A*, Fluorescent caveolin-1-mCherry (*red*) was expressed in HeLa cells by lentiviral gene transfer. *B*, Caveolin-1 was labeled using an anti-caveolin-1 antibody and Alexa Fluor 488–conjugated secondary antibody (*green*). *C*, The merged image shows colocalization of caveolin-1 and the additionally expressed caveolin-1-mCherry. *D*, Caveolin-1–enhanced green fluorescent protein (EGFP)-expressing HeLa cells were exposed to EBOV-VLPs-Cy5 at 4°C followed by a temperature shift to 37°C. Live cell imaging was performed, and time-dependent 3-dimensional stacks were acquired followed by 3-dimensional reconstruction. No colocalization of EBOV-VLPs (*red*) or caveolin-1-EGFP (*green*) was observed. *E*, HeLa cells were exposed to EBOV-VLPs for 1 hour at 4°C followed by a 15-minute temperature shift to 37°C, fixed, and stained for caveolin-1 and EBOV-VLPs using an antibody directed against $GP_{1,2}$. Most of the VLPs were not colocalized (insert, *red*), but a very few VLPs overlapped with cav-1 staining (insert, *yellow*) *F*, Cholera toxin B (CTx-B) served as a positive control and colocalized with caveolin-1. Scale bar: 5 μm.

DISCUSSION

Viruses developed a number of strategies to enter target cells. These include endocytosis via clathrin-coated pits, caveolae, nonclathrin/noncaveolae–mediated processes, phagocytosis, and macropinocytosis [10, 43]. The classical clathrin- or caveolin-1 mediated endocytotic vesicles are commonly smaller than 200 nm and 100 nm, respectively [18, 19]. Thus, it seems reasonable to assume that the large EBOV particles use other mechanisms for cellular entry, such as macropinocytosis. Macropinocytosis refers to formation of macropinosomes, which are large endocytotic vesicles formed at specific locations of the plasma membrane. This process is suited for uptake of extracellular material such as fluid, antigens, or even large apoptotic cells [11]. Here we have identified a macropinocytosis-like process as the critical mechanism for EBOV particle uptake into target cells. This discovery is consistent with findings in 2 very recent reports that were performed concomitantly with our work [44, 45].

In our study we could demonstrate that several hallmarks of macropinocytosis, such as local actin polymerization leading to ruffle formation, activation of the PI3-kinase pathway, and the Na+/H+-exchanger activity, were associated with the uptake of the majority of EBOV particles into cells (Figure 4). In particular, the uptake was significantly reduced by the inhibition of the Na+/H+-exchanger activity, which is known to be critical for macropinocytosis [10]. The finding that latrunculin A had a weaker effect on particle uptake might be due to 2 phenomena. First, depolymerization of actin filaments results in cell rounding and cell detachment [46]. In order to avoid those processes, latrunculin A had to be used at lower concentrations that only partially block actin polymerization and thus may still allow limited entry of particles. Second, a smaller number of particles might enter the cells by a different mechanism such as clathrin-mediated uptake as identified here (Figure 5), a phenomenon that might be related to differences in particle size. Particle heterogeneity has been shown for both infectious EBOV and noninfectious EBOV-VLPs [1, 17, 20, 47]. Two modes of clathrin coat formation have been described: the classical small clathrin-coated pits, which form rapidly and mediate fast uptake, and the larger coated plaques, which are longer-lived structures

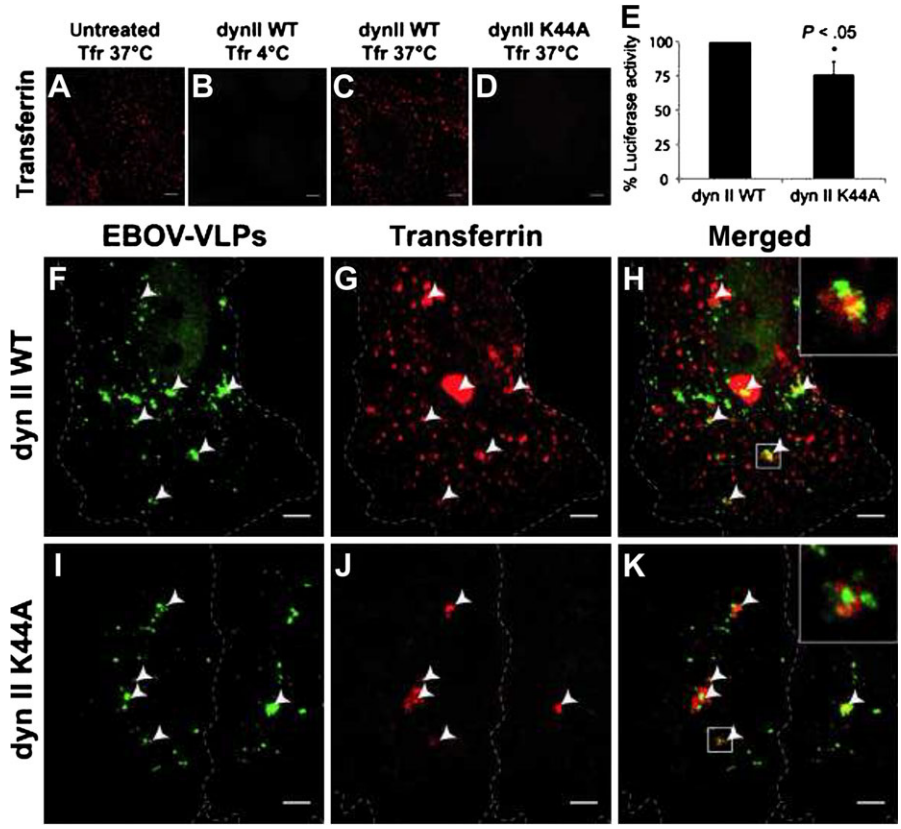

Figure 7. Dynamin II modulates Ebola virus-like particle (EBOV-VLP) uptake in HeLa cells. Dynamin II-WT (dynII WT) and a dynamin II-K44A mutant (dynII K44A) were expressed in HeLa cells to block both caveolin-1 and clathrin-mediated endocytosis, and subsequently tested for the ability to take up EBOV-VLPs, or transferrin (positive control). *A–D,* HeLa cells expressing either dynamin II-WT or dynamin II-K44A mutant were exposed to transferrin–Alexa Fluor 546 at temperatures indicated. There was no transferrin uptake in cells expressing the dynamin II K44A mutant. *E,* HeLa cells expressing either dynamin II or dynamin II-K44A were infected with EBOV-iVLPs and analyzed for *Renilla* luciferase activity after 70 hours. There was 25% downregulation of luciferase activity in dynamin II-K44A–expressing cells. *F–K,* HeLa cells expressing dynamin II-WT (*F–H*) or dynamin II K44A mutant (*I–K*) were exposed to EBOV-VLPs for 60 minutes and to transferrin–Alexa Fluor 546 for 15 minutes and fixed, and EBOV-VLPs (*green*) were stained for $GP_{1,2}$. *F–H,* Some EBOV-VLPs were found in exceptionally large transferrin-positive vesicles, while the bulk of EBOV-VLPs did not colocalize with transferrin. *I–K,* In contrast, HeLa cells expressing dynamin II-K44A were negative for the characteristic small transferrin-positive vesicles, but still showed the exceptionally large EBOV-VLP–containing macropinosomes. Arrowheads indicate colocalized structures as indicated. Experiment was repeated 3 times. Error bars represent standard errors. Scale bars: 5 μm.

depending on actin dynamics and differing in uptake velocity and mechanisms [48]. Clathrin-mediated uptake of large pathogens was previously described for *Listeria monocytogenes* that use planar clathrin-coated plaques [49]. Therefore, the uptake of some EBOV particles appears to be clathrin-mediated but independent of the classical clathrin-mediated pathway.

As with several other viruses, EBOV particles appear to be internalized by more than 1 endocytotic pathway. Although 2 other studies showed that clathrin does not play a role in EBOV entry of Vero cells, our data indicate that in HeLa cells clathrin does contribute to particle internalization. Based on published data and the results reported here, we assume that the endocytotic pathways taken by EBOV particles may differ depending on the cell type and origin. In addition, EBOV particle size might determine the entry mechanism. The latter might explain the results of studies using HIV particles pseudotyped with EBOV-$GP_{1,2}$ with an estimated size of about 100 nm, which were internalized in a clathrin-dependent fashion [14]. This is in accordance with recent reports showing that chlorpromazine, a drug that alters a wide variety of cellular mechanisms including certain types of endocytosis [50, 51], inhibited the uptake of infectious EBOV [14]. The impact of clathrin on EBOV particle uptake is also consistent with the inhibitory effect of the dynamin II-K44A mutant, which is known to block clathrin- and caveolae-mediated endocytosis (Figure 7).

In summary, it appears that EBOV particle uptake occurs by various pathways and depends among other factors on the host cell and virus particle size. However, macropinocytosis and, to a certain degree, clathrin-mediated endocytosis seem to be the main mechanisms for particle uptake into cells.

Supplementary Data

Supplementary Data are available at *The Journal of Infectious Diseases* online.

Funding

This work was supported by the Deutsche Forschungsgemeinschaft (SCHN 430/3-3 and SCH 430/6-1), the Schering foundation (N. B., T. H.), the Public Health Agency of Canada, the Intramural Research Program of the National Institutes of Health, and the Center for Regenerative Therapy Dresden.

Acknowledgments

We thank Sylvia Großklaus for excellent technical assistance. Yoshihiro Kawaoka, University of Wisconsin–Madison, kindly provided Ebola-specific antibodies and Yvan Arsenijevic (Lausanne, Switzerland) the pFUGW vector. Paulina Aleksandrowicz and Hans Schnittler are grateful to Kai Simons and Michele Solimena (Dresden, Germany) for their advisory role on Paulina's thesis committee through the Dresden International Graduate School for Biomedicine and Biotechnology.

References

1. Sanchez A, Geisbert TW, Feldmann H. Marburg and Ebola viruses. In: Fields BN, Knipe DM, Howley PM, eds. Fields virology. 5th ed. Philadelphia: Wolters Kluwer Health/Lippincott Williams & Wilkins, 2007.
2. Feldmann H, Jones S, Klenk HD, Schnittler HJ. Ebola virus: from discovery to vaccine. Nat Rev Immunol **2003**; 3:677–85.
3. Geisbert TW, Jahrling PB. Exotic emerging viral diseases: progress and challenges. Nat Med **2004**; 10:S110–21.
4. Schnittler HJ, Feldmann H. Marburg and Ebola hemorrhagic fevers: does the primary course of infection depend on the accessibility of organ-specific macrophages? Clin Infect Dis **1998**; 27:404–6.
5. Feldmann H, Volchkov VE, Volchkova VA, Stroher U, Klenk HD. Biosynthesis and role of filoviral glycoproteins. J Gen Virol **2001**; 82:2839–48.
6. Takada A, Watanabe S, Ito H, Okazaki K, Kida H, Kawaoka Y. Downregulation of beta1 integrins by Ebola virus glycoprotein: implication for virus entry. Virology **2000**; 278:20–6.
7. Alvarez CP, Lasala F, Carrillo J, Muniz O, Corbi AL, Delgado R. C-type lectins DC-SIGN and L-SIGN mediate cellular entry by Ebola virus in cis and in trans. J Virol **2002**; 76:6841–4.
8. Shimojima M, Ikeda Y, Kawaoka Y. The mechanism of Axl-mediated Ebola virus infection. J Infect Dis **2007**; 196(Suppl 2):S259–63.
9. Becker S, Spiess M, Klenk HD. The asialoglycoprotein receptor is a potential liver-specific receptor for Marburg virus. J Gen Virol **1995**; 76:393–9.
10. Mercer J, Helenius A. Virus entry by macropinocytosis. Nat Cell Biol **2009**; 11:510–20.
11. Swanson JA. Shaping cups into phagosomes and macropinosomes. Nat Rev Mol Cell Biol **2008**; 9:639–49.
12. Empig CJ, Goldsmith MA. Association of the caveola vesicular system with cellular entry by filoviruses. J Virol **2002**; 76:5266–70.
13. Yonezawa A, Cavrois M, Greene WC. Studies of Ebola virus glycoprotein-mediated entry and fusion by using pseudotyped human immunodeficiency virus type 1 virions: involvement of cytoskeletal proteins and enhancement by tumor necrosis factor alpha. J Virol **2005**; 79:918–26.
14. Bhattacharyya S, Warfield KL, Ruthel G, Bavari S, Aman MJ, Hope TJ. Ebola virus uses clathrin-mediated endocytosis as an entry pathway. Virology **2010**; 401:18–28.
15. Sanchez A. Analysis of filovirus entry into vero e6 cells, using inhibitors of endocytosis, endosomal acidification, structural integrity, and cathepsin (B and L) activity. J Infect Dis **2007**; 196(Suppl 2):S251–8.
16. Saeed MF, Kolokoltsov AA, Freiberg AN, Holbrook MR, Davey RA. Phosphoinositide-3 kinase-Akt pathway controls cellular entry of Ebola virus. PLoS Pathog **2008**; 4:e1000141.
17. Feldmann H, Geisbert TW, Jahrling PB, et al. Filoviridae. In: Fauquet CM, Mayo MA, Maniloff J, Desselberger U, Ball LA, eds. Virus taxonomy: VIIIth report of the International Committee on Taxonomy of Viruses. London: Elsevier Academic Press, 2005; 645–53.
18. Richter T, Floetenmeyer M, Ferguson C, et al. High-resolution 3D quantitative analysis of caveolar ultrastructure and caveola-cytoskeleton interactions. Traffic **2008**; 9:893–909.
19. Traub LM. Clathrin couture: fashioning distinctive membrane coats at the cell surface. PLoS Biol **2009**; 7:e1000192.
20. Noda T, Sagara H, Suzuki E, Takada A, Kida H, Kawaoka Y. Ebola virus VP40 drives the formation of virus-like filamentous particles along with GP. J Virol **2002**; 76:4855–65.
21. Wahl-Jensen VM, Afanasieva TA, Seebach J, Stroher U, Feldmann H, Schnittler HJ. Effects of Ebola virus glycoproteins on endothelial cell activation and barrier function. J Virol **2005**; 79:10442–50.
22. Hoenen T, Groseth A, Kolesnikova L, et al. Infection of naive target cells with virus-like particles: implications for the function of Ebola virus VP24. J Virol **2006**; 80:7260–4.
23. Seebach J, Donnert G, Kronstein R, et al. Regulation of endothelial barrier function during flow-induced conversion to an arterial phenotype. Cardiovasc Res **2007**; 75:596–607.
24. Ebihara H, Theriault S, Neumann G, et al. In vitro and in vivo characterization of recombinant Ebola viruses expressing enhanced green fluorescent protein. J Infect Dis **2007**; 196(Suppl 2):S313–22.
25. Helenius A, Kartenbeck J, Simons K, Fries E. On the entry of Semliki forest virus into BHK-21 cells. J Cell Biol **1980**; 84:404–20.
26. Pelkmans L, Kartenbeck J, Helenius A. Caveolar endocytosis of simian virus 40 reveals a new two-step vesicular-transport pathway to the ER. Nat Cell Biol **2001**; 3:473–83.
27. Altschuler Y, Barbas SM, Terlecky LJ, et al. Redundant and distinct functions for dynamin-1 and dynamin-2 isoforms. J Cell Biol **1998**; 143:1871–81.
28. Kostic C, Chiodini F, Salmon P, et al. Activity analysis of housekeeping promoters using self-inactivating lentiviral vector delivery into the mouse retina. Gene Ther **2003**; 10:818–21.
29. Soulet F, Schmid SL, Damke H. Domain requirements for an endocytosis-independent, isoform-specific function of dynamin-2. Exp Cell Res **2006**; 312:3539–45.
30. Schindelin J. Fiji Is Just ImageJ–batteries included. Luxembourg: ImageJ User and Developer Conference, **2008**.
31. Kalaidzidis Y. Intracellular objects tracking. Eur J Cell Biol **2007**; 86:569–78.
32. Afanasieva TA, Wahl-Jensen V, Seebach J, et al. Hemorrhagic fevers: endothelial cells and Ebola-virus hemorrhagic fever. In: Aird WC, ed. Endothelial biomedicine. New York: Cambridge University Press, 2007; 1311–9.
33. Spector I, Shochet NR, Kashman Y, Groweiss A. Latrunculins: novel marine toxins that disrupt microfilament organization in cultured cells. Science **1983**; 219:493–5.
34. Vigne P, Frelin C, Cragoe EJ Jr, Lazdunski M. Ethylisopropylamiloride: a new and highly potent derivative of amiloride for the inhibition of the Na+/H+ exchange system in various cell types. Biochem Biophys Res Commun **1983**; 116:86–90.
35. Wymann MP, Bulgarelli-Leva G, Zvelebil MJ, et al. Wortmannin inactivates phosphoinositide 3-kinase by covalent modification of Lys-802, a residue involved in the phosphate transfer reaction. Mol Cell Biol **1996**; 16:1722–33.
36. Parton RG. Caveolae meet endosomes: a stable relationship? Dev Cell **2004**; 7:458–60.
37. Bavari S, Bosio CM, Wiegand E, et al. Lipid raft microdomains: a gateway for compartmentalized trafficking of Ebola and Marburg viruses. J Exp Med **2002**; 195:593–602.

38. Praefcke GJ, McMahon HT. The dynamin superfamily: universal membrane tubulation and fission molecules? Nat Rev Mol Cell Biol **2004**; 5:133–47.
39. Schlunck G, Damke H, Kiosses WB, et al. Modulation of Rac localization and function by dynamin. Mol Biol Cell **2004**; 15:256–67.
40. Bonazzi M, Spano S, Turacchio G, et al. CtBP3/BARS drives membrane fission in dynamin-independent transport pathways. Nat Cell Biol **2005**; 7:570–80.
41. Lindemann D, Schnittler H. Genetic manipulation of endothelial cells by viral vectors. Thromb Haemost **2009**; 102:1135–43.
42. Le Roy C, Wrana JL. Clathrin- and non-clathrin-mediated endocytic regulation of cell signalling. Nat Rev Mol Cell Biol **2005**; 6:112–26.
43. Marsh M, Helenius A. Virus entry: open sesame. Cell **2006**; 124:729–40.
44. Nanbo A, Imai M, Watanabe S, et al. Ebolavirus is internalized into host cells via macropinocytosis in a viral glycoprotein-dependent manner. PLoS Pathog **2010**; 6:e1001121.
45. Saeed MF, Kolokoltsov AA, Albrecht T, Davey RA. Cellular entry of Ebola virus involves uptake by a macropinocytosis-like mechanism and subsequent trafficking through early and late endosomes. PLoS Pathog **2010**; 6:e1001110.
46. Schnittler HJ, Schneider SW, Raifer H, et al. Role of actin filaments in endothelial cell-cell adhesion and membrane stability under fluid shear stress. Pflugers Arch **2001**; 442:675–87.
47. Wahl-Jensen V, Kurz SK, Hazelton PR, et al. Role of Ebola virus secreted glycoproteins and virus-like particles in activation of human macrophages. J Virol **2005**; 79:2413–9.
48. Saffarian S, Cocucci E, Kirchhausen T. Distinct dynamics of endocytic clathrin-coated pits and coated plaques. PLoS Biol **2009**; 7:e1000191.
49. Cossart P, Veiga E. Non-classical use of clathrin during bacterial infections. J Microsc **2008**; 231:524–8.
50. Sieczkarski SB, Whittaker GR. Dissecting virus entry via endocytosis. J Gen Virol **2002**; 83:1535–45.
51. Vercauteren D, Vandenbroucke RE, Jones AT, et al. The use of inhibitors to study endocytic pathways of gene carriers: optimization and pitfalls. Mol Ther **2010**; 18:561–9.